A ROUND ROBIN TEST OF A LOW-PRESSURE AXIAL FAN

Michail VOURAKIS[1], Mikael KARLSSON[2]

[1] *Chalmers University of Technology, Department of Mechanics and Maritime Sciences, Division of Fluid Dynamics, Hörsalsvägen 7A SE-412 96 Gothenburg, Sweden*

[2] *KTH Royal Institute of Technology, Department of Engineering Mechanics, The Marcus Wallenberg Laboratory for Sound and Vibration Research, Teknikringen 8, 100 44 Stockholm, Sweden*

SUMMARY

The reproducibility of aerodynamic and aeroacoustic results on a benchmark low-pressure axial fan is discussed. Growth of interest in this type of fans due to the new demands for cooling of electrified powertrains in the automotive industry, is the motivator of this study. The publicly available geometry and setup documented by Zenger *et al.* [1] is utilized. Included results demonstrate high repeatability among the three 3D printed copies of the fan with regards to manufacturing, aerodynamic and acoustic performance over multiple operating points. Moreover, good reproducibility is achieved at the design point concerning the main acoustic and aerodynamic performance characteristics of the fan. Deviations are observed at the stall region suggesting the need of further investigations, including the effects of installation and non-ideal acoustic environment.

INTRODUCTION

In recent years the automotive industry is pushing towards a rising production of electric vehicles. The replacement of the internal combustion system has led to the reinvention of several systems closely linked to its performance. Cooling systems are among the latter, due to the different operating scenarios and overall needs of an electric motor. Consequently, to meet the requirements of said systems testing and optimization of their core components like fans is vital. A testing rig facility where the main aerodynamic and acoustic performance characteristics of candidate fan designs are evaluated, is a significant enabler to this end.

This brings us to the purpose of this study, the assessment of a testing facility and measurement methods for acoustic and aerodynamic performance of axial fans. To facilitate the latter a

benchmark low-pressure axial fan was utilized. Zenger *et al*. [1] have published and made publicly available the geometry of the fan and test setups/methods to make it possible to reproduce their results. Different copies of fan were 3D printed to see variations one can expect from small production differences and a wide range of operating points were measured to verify repeatability. Initially additional measurements were planned in an established test facility where detailed flow field measurements are feasible. However, non-conclusive results from the latter at this stage, limit this discussion for now on results from one testing facility.

Firstly, the testing facility implemented is introduced followed by the measurement setups, instrumentation and measurement settings implemented. Subsequently, the manufacturing along with the main indicators of aerodynamic and acoustic performance of the 3D printed fans are discussed. The study ends with the main conclusions drawn and suggestions for further work.

EXPERIMENTAL SETUP

All experimental investigations were carried out in the closed loop Fan Test Rig at the industrial partner Volvo GTT. Figure 1 gives a schematic of the test rig's layout.

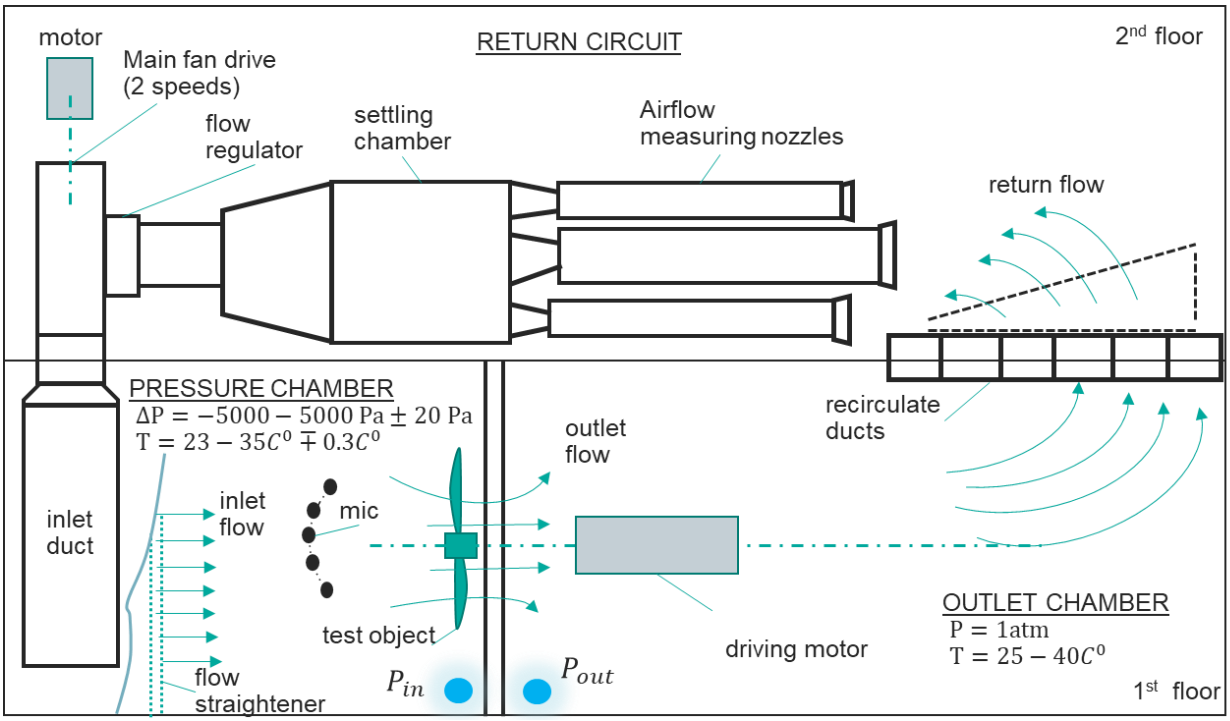

Figure 1: Schematic of fan test rig

The air flow goes through the pressure chamber where the fan-test object is installed and exits at the outlet chamber where the driving motor of the fan is located. A side outlet within the outlet chamber guides the flow to the second floor of the rig where the return circuit is situated. The latter consists of a nozzle-valve system which along with a compensation fan regulates the volumetric flow. The ISO 5167-1 (2003) standard is implemented for calculating the flow rate from measurements registered by the venturi nozzles. Pressure sensors upstream and downstream the fan-test object provide the differential pressure between pressure chamber and ambient conditions. More information about the operation of the fan test rig and measurement accuracy of principal parameters may be found at [2,3].

Sound field measurements were carried upstream of the fan, within the pressure chamber. The pressure chamber has been retrofitted with acoustic absorbers except for the floor and the interface between pressure and outlet chamber. That improved the overall room acoustics, like critical distance and reverberation time, towards a semi-anechoic environment. It should be noted here that

due to the proximity of the facility to other testing facilities, background noise of significant amplitude can be observed at frequencies below 200 Hz. Thereby in this study, the lower frequency limit for meaningful analysis has been set to that value.

Instrumentation

Information about the design parameters of the fan implemented can be found at [1]. The fan along with its stator and shroud were 3D printed via laser sintering machine EOS P770. The 3D printing material was polyamide PA12. Three examples of the fan were 3D printed. The manufacturing process was evaluated by scanning the fans and comparing their dimensions to the CAD (computer aided design) model. The scanning equipment utilized for the latter was ATOS Tripe Scan, while post processing was performed by Polyworks of InnovMetric.

The sound field of the fan was measured with 101 ¼ inch free- field array microphones (type GRAS 40PH). Windscreens were utilized to reduce effect of flow noise, during the fan's operation. The microphones were arranged in nine arcs, each spanning over 120^o angle. Two different measurement surfaces were utilized. The first comprised of five arcs centered around the fan's rotation center. Distance was set at 1 m radius. The polar spacing (height) between consecutive arcs was 20^o angle. Each arc contained thirteen microphones spaced 10^o apart (azimuth direction). The second measurement surface of four arcs, was placed at 1.5 m radius, while the microphone (mic) spacing along each arc was 15^o. The polar spacing was same as group 1. Figure 2 contains a graphic representation of the mic grid in relation to the center of rotation and grid angles, as well as the final measurement setup.

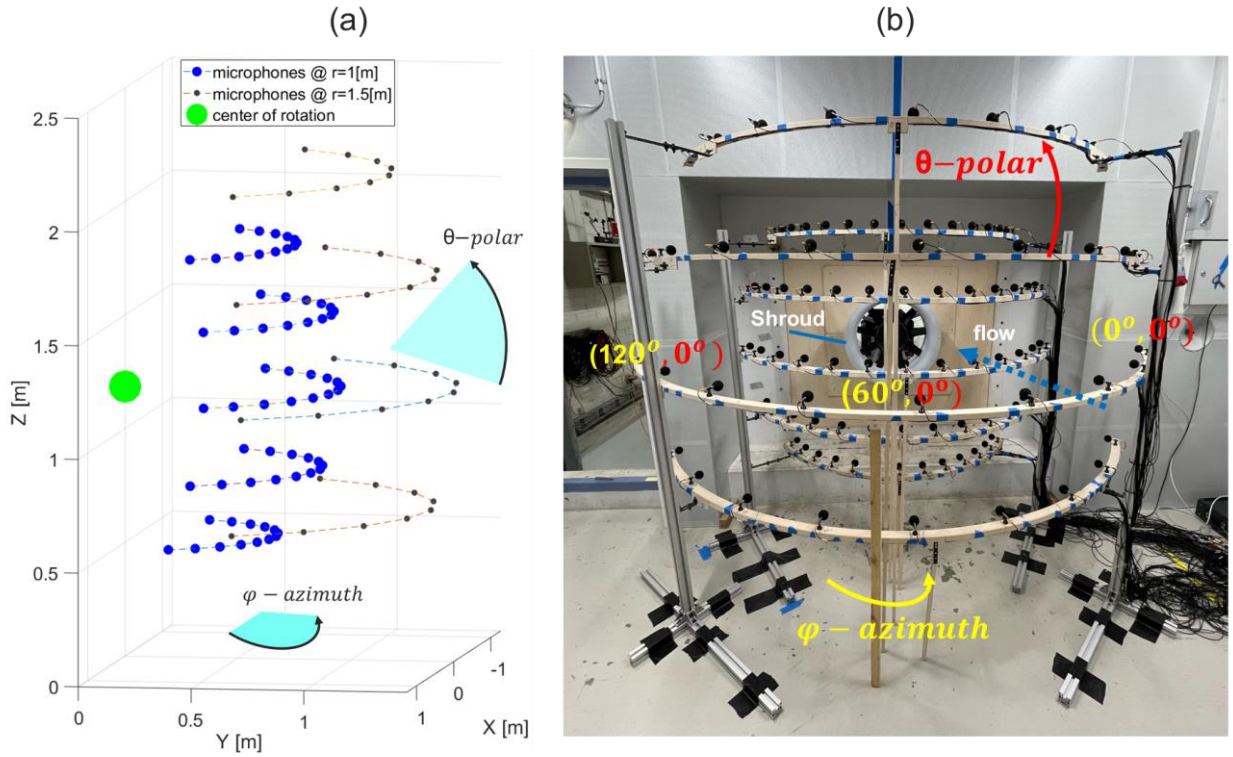

Figure 2: Mic grid; (a) Schematic of mic positions relative to center of rotation, (b) Installation setup

The employed measurement grid was a product of the pressure room's acoustic, number of available sensors, spatial resolution, as well as additional investigation objectives which will not be analyzed in this study. Due to space irregularities an environment correction factor K_2 was calculated for both measurement surfaces. The reverberation method for a half-hemisphere measurement surface [4] was implemented. K_2 values of 0.9 dB and 1.8 dB were calculated for the measurement surfaces at 1 m and 1.5 m respectively.

The frame supporting the microphones is expected to introduce scattering effects to the radiated sound field at higher frequencies when the wavelengths are comparable to its dimensions. Considering that its thickness was reduced to the minimum allowable level, limited by the structure's rigidity and the need to accommodate the wires of the microphones.

The rotational speed of the motor's shaft, which was directly connected to the fan's hub disk, was measured internally via a trigger sensor, as well as a digital laser tachometer in sync with the acoustic measurements. The torque of the motor was measured with a torque meter. A calibration measurement was done without the fan installed. This allowed the estimation of torque imposed by the inherent friction of the bearings, which was subsequently removed from data recorded for the fan.

The data acquisition system Simcenter SCADAS Mobile was used for handling the signals of the microphones, and tachometer.

Measurement settings

The sampling frequency of the mic and tachometer signals was 51.2 kHz. Measurement time of each fan operating point was 30 seconds, while the linear spectra were calculated using MATLAB's pwelch function (version R2019b). Hanning window was implemented with 50 % overlapping and 2^{16} sample points.

The total-to-static efficiency η_{ts} was then calculated according to [1]:

$$\eta_{ts} = \frac{\dot{V}\Delta p_{ts}}{2\pi nT} \quad (1)$$

Where, $\dot{V}$ is the volumetric flow rate in m^3/s, Δp_{ts} is the pressure difference total-to-static in Pa, n is the rotational speed in s^{-1} and T the motor's torque in Nm. It should be noted here that the pressure chamber has a considerable higher cross section (~3.2 m) compared to the fan's diameter (~0.5 m). Then it is common practice to assume that the pressure difference between pressure chamber and ambient (pressure measured in outlet chamber) is the total-to-static pressure difference.

The sound power level (SWL) was calculated for each measurement surface according to [4]:

$$SWL = \widetilde{L_p} + 10\log\left(\frac{S}{S_0}\right) \quad (2)$$

Where, $\widetilde{L_p}$ is the spatial average of the sound pressure level (SPL) for each measurement surface after the environment correction. S is the measurement surface corresponding to microphones at 1 m or 1.5 m (3.14 and 7.06 m^2), while S_0 is a reference surface set to 1 m^2. There was no need for background noise correction.

RESULTS

Manufacturing assessment

The deviation of the 3D printed fans from the CAD model is given in Figure 3. The depicted images refer to the front view of the fan (flow towards paper). Overall, all fans register similar levels of fluctuations from the CAD model. The distribution of fluctuations is not uniform across different blades for all fans. However maximum positive deviations, around 1.5 mm, are mainly observed towards the blade tips for all 3D printed cases. In contrast the minima are mainly found close to the hub for all fans.

To further investigate the extent of the deviations, the fans were scanned from the other direction. This verified that the material thickness was consistent across all fans. Thereby it was concluded that the observed maxima over certain blades, represented a ''mild'' bending, corresponding to 2^o in

the worst-case scenario. Taking also into account the suitability of the material, the manufacturing process of the fan is highly repeatable.

The remaining parts of the fan assembly, comprising of the shroud and the stator were not scanned as one example was used for all fans. It should be acknowledged that the assembly of the shroud and stator across the interface wall separating pressure chamber and outlet chamber, was not flawless. The shroud was 3D printed as a three-piece part, comprising the bell mouth entry section, straight duct section and outlet duct section. Sanding along the boundary interfaces of consecutive sections was performed to minimize assembling asymmetries. Still the tip clearance was not constant across the circumference, registering 0.5 mm deviations at certain angles.

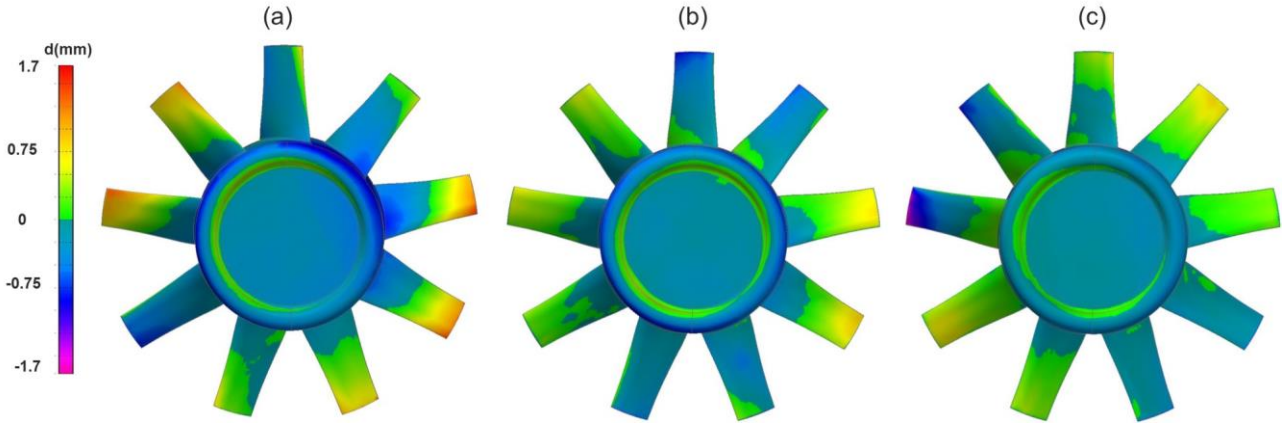

Figure 3: Deviation (d) of 3D printed fans from CAD model;
(a) Fan A, (b) Fan B, (c) Fan C

Aerodynamic performance assessment

The aerodynamic characteristic curves of the three 3D printed fans are given in Figure 4. The respective curves of the benchmark case [1] are also included (denoted as Ref). Rotational speed is 1486 rpm.

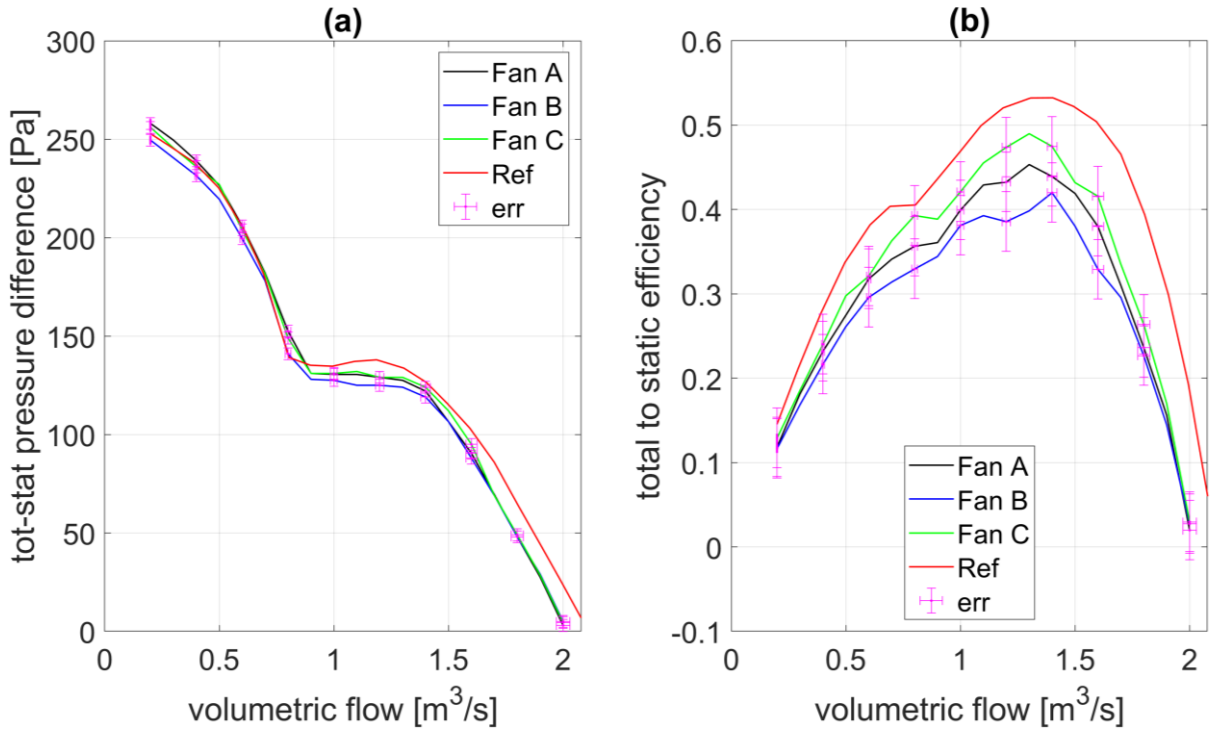

Figure 4: Aerodynamic characteristic curves at 1486rpm; (a) Pressure difference, (b) Efficiency

Regarding the pressure curve there is good repeatability between the different 3D printed fans. Maximum differences fall within the range of measurement error (± 3 Pa for pressure, 1.5 % flow rate). Compared to the reference data the curves agree qualitatively, showcasing the same starting point of stall condition. Maximum deviations occur before the design point (1.4 m^3/s) within the stall region and reach 3 % for the 3D printed fan closer to the reference data curve.

The efficiency showcases qualitative agreement across the 3D printed fans and the reference curve. However, the calculated values from the 3D printed fans are overall underestimated compared to the reference. The resulting uncertainty of the calculated efficiency is higher, since pressure, torque and volumetric flow contribute (Eq. 1). Moreover, in this measurement scenario the overall low torque values needed, translated into higher than anticipated uncertainty for the torque readings. It should also be noted here that performed measurements at a separate test facility showcased unreliable results with regards to the fan's efficiency. Hence, future measurements are planned to investigate the lack of quantitative reproducibility.

Besides the design point for which data from the reference case [1] was available, more rotational speeds were measured. Figure 5 includes the aerodynamic characteristic curves for all rotational speeds measured. The fans maintain the quantitative agreement with regards to pressure rise as the rotational speed decrease. The efficiency curves deviate more across the three fans. However, deviations remain largely within the measurement uncertainty.

Consecutive measurements with the same fan, after a time span of two weeks, produced characteristic curves well within the measurement uncertainty of the test rig [3].

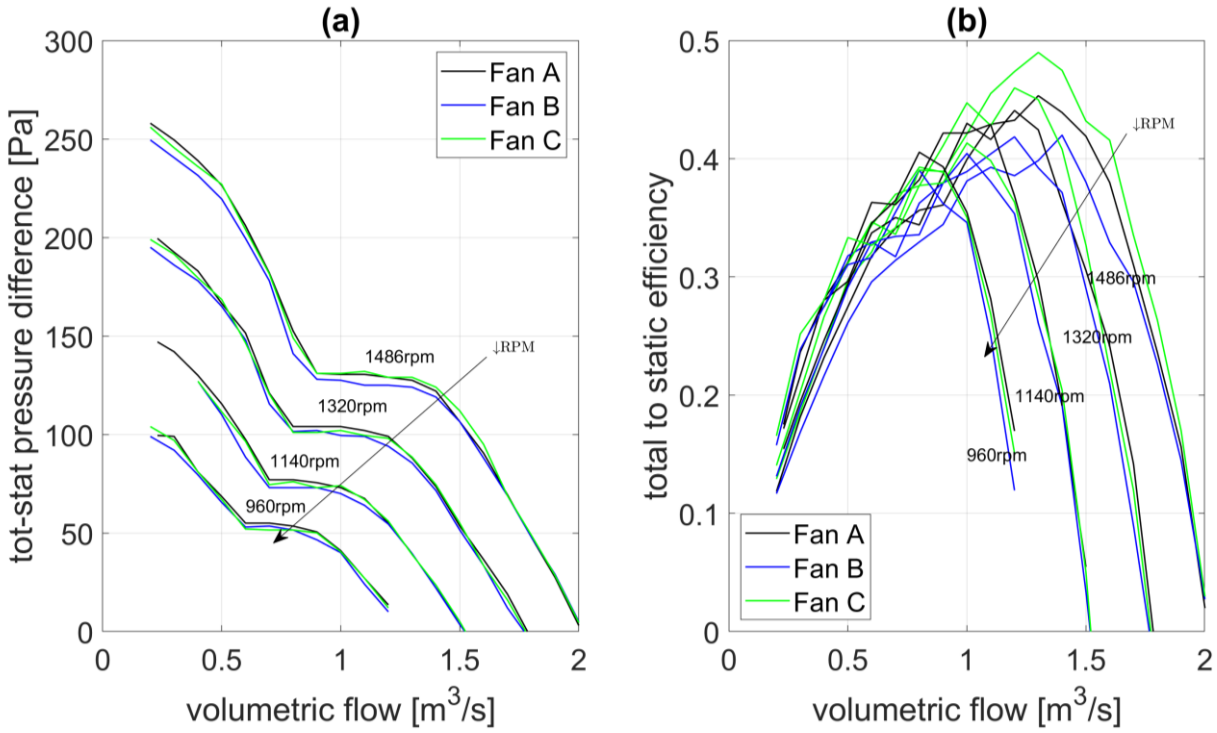

Figure 5: Aerodynamic characteristic curves at different rotational speeds; (a) Pressure difference, (b) Efficiency

Acoustic performance assessment

The sound power spectrum (Eq. 2) of the 3D printed fans at the design point is given in Figure 6. Once again, the reference data [1] is superimposed. Spectra are calculated from microphones at 1 m distance from fan's center of rotation. The upper frequency limit has been set to 2 kHz.

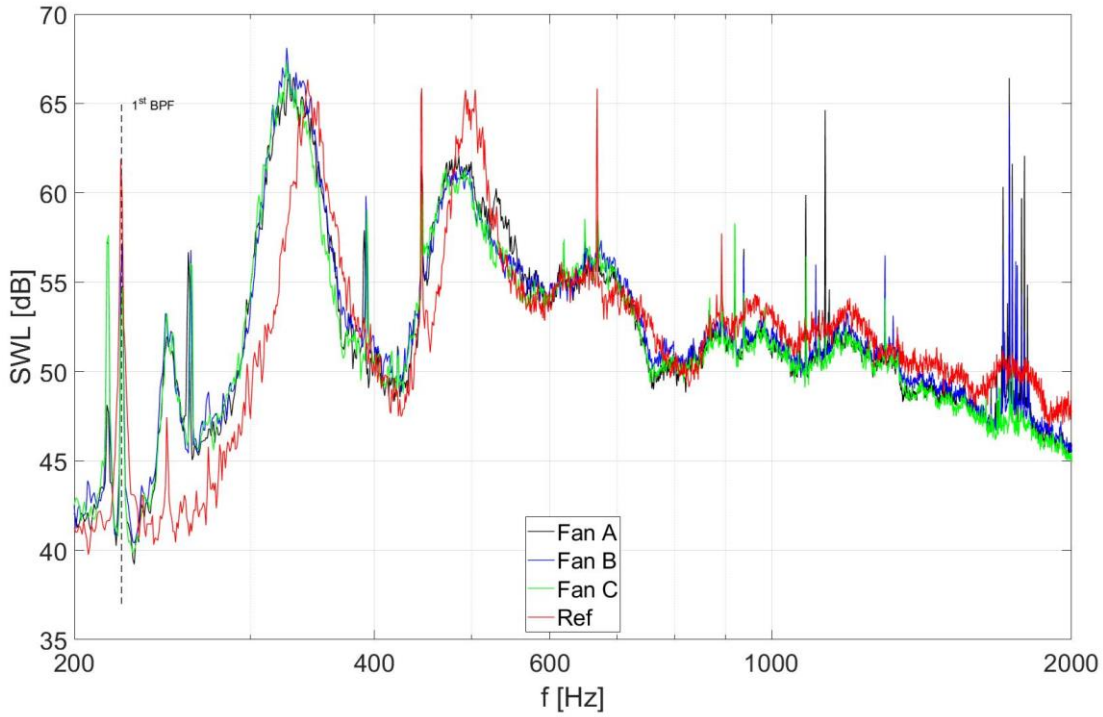

Figure 6: Sound power spectra of 3D printed fans and reference at 1486 rpm, 1.4 m^3/s

The reason for this decision was the observation of noise components associated with the bearings of the driving motor. The first tonal component of the spectra, before the 1st BPF is such an example. Since comparable noise levels were recorded for the motor running with and without the fan over 4 kHz, the upper limit of the analysis was set at 2 kHz. Still the frequency range depicted in Figure 6 contains most important part of the spectra, which mainly contribute to the total SWL of this fan.

The spectra of all 3D printed fans agree well throughout the frequency range. Compared to the reference all peaks below 300 Hz are in phase. The latter includes the first blade passing frequency (~225 Hz). At frequencies close to the highest amplitudes of the spectra (~320 Hz), the reference data demonstrate a frequency shift. This section of the spectra is associated with flow noise due to the blade tip and shroud interaction. As stated in previous section, the final installation did not produce a constant blade tip clearance, possibly explaining the deviation from the reference. Still the phenomenon is captured. At higher frequencies spectra from all 3D printed fans showcase distinct peaks, probably related to bearing noise contribution or other background noise source which has not been identified.

Calculation of the total SWL, within the stated frequency range, gives the values which are included in Table 1 for the two measurement surfaces.

Table 1: total SWL of 3D printed fans and reference [1]

	total SWL – mic @ 1 m [dB]	**total SWL – mic @ 1.5 m [dB]**
Fan A	87.5	86.6
Fan B	87.7	86.7
Fan C	87.1	86.1
Reference	87.8	-

As expected from the similarity of the narrowband sound power spectra, the total levels are very close between the 3D printed fans and from the reference data [1], not more than 1 dB for the closest measurement surface. In addition, total SWL calculated from the furthest measurement surface are within close range. Results from repeated measurements for the same fan were within 0.4 dB from a SWL standpoint.

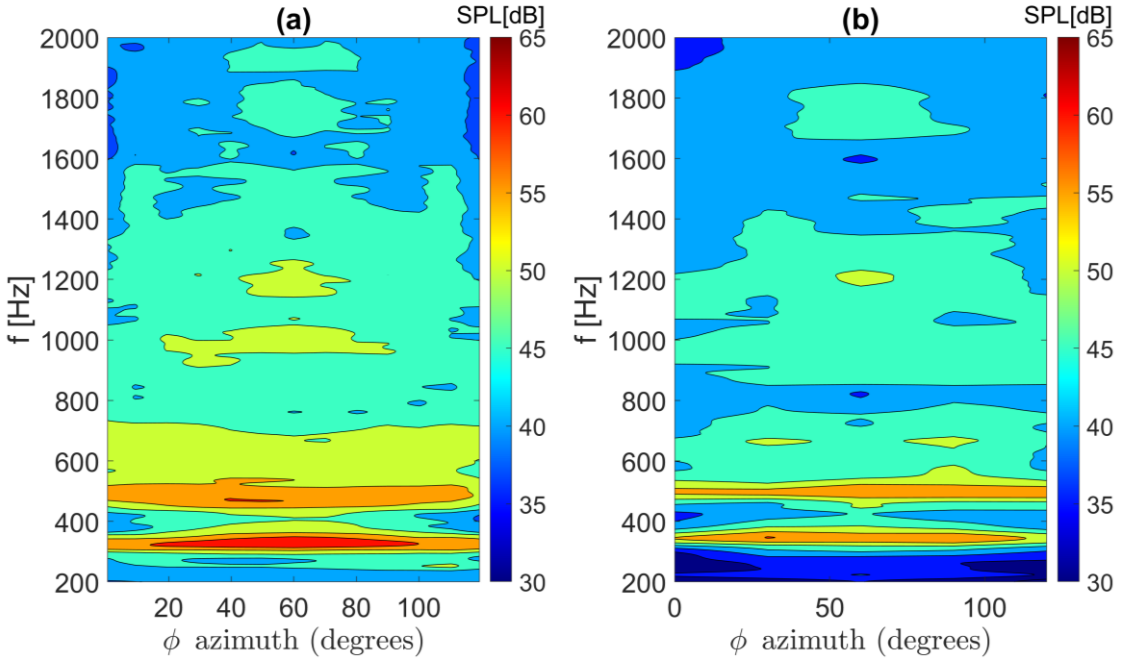

Figure 7: SPL distribution over azimuth angle and frequency at 0^o polar angle; (a) Fan C, (b) Reference

Another aspect worth investigating is the directivity of the acoustic field. Figure 7 showcases the SPL spectra over the azimuth angle for microphones at the same height as the center of rotation and 1 m distance. Since all 3D fans demonstrated quantitatively similar SPL distribution, one case is compared to the reference data. Initially it is observed that the acoustic field of the 3D printed fan is relatively symmetric over the azimuth. Highest amplitudes are found close to the centerline (60^o) consistently across all frequencies. The acoustic behavior of the 3D printed fan verifies the reference data at a great extent qualitatively, although the latter measurements were made in an anechoic chamber. This is also the case for lower frequencies, within the 220 - 450 Hz range where the highest amplitudes are registered. At these frequencies the non-ideal acoustic environment is expected to interfere by introducing reflections. However, from the perspective of azimuth angle its contribution appears to be uniform.

Finally, the sound characteristic map of the 3D printed fans is estimated. This entails sound characteristic curves (total SWL over volume flow rate) for different rotational speeds, depicted in Figure 8. Reference data are only available for rotational speed of 1486 rpm and concern frequency range of 100 – 10000 Hz. Since the majority of the total SWL is included up to 2 kHz, the available values from [1] at different volume flow rates, have been adjusted based on the calculated total SWL of the reference data (200 - 2000 Hz) at the design point.

The 3D printed fans agree well below the 1.4 m³/s mark for the depicted rotational speeds. At flow rates closer to the maximum attainable airflow the total SWL stagnates, while the biggest deviations across the fans are registered. However, at these flow rates the fan hardly produces any pressure rise and the total SWL dependence to blade tip noise should increase [6].

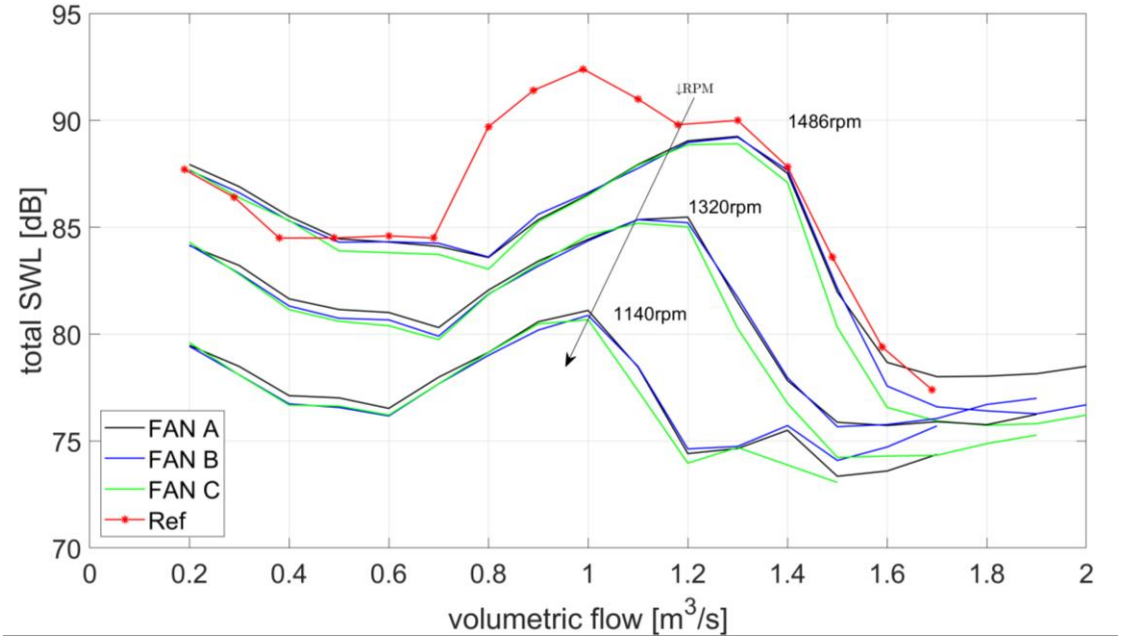

Figure 8: Sound characteristic map of 3D printed fans at different rotation speeds and reference data at 1486rpm

Thereby, the differences of tip clearance across the 3D printed fans, due to the installation, are possibly the main reason of discrepancies. This stagnation of sound spectra at high flow rates for this fan design has also been observed at [5], implying reproducibility of the phenomenon.

For the rotational speed of 1486 rpm good agreement between reference and 3D printed fans is achieved, for flow rates close to the design point and below 0.7 m³/s towards the no flow point. However, for interim flow rates deviations are significant. These interim flow rates span over the stall region of the aerodynamic curve (Figure 4). Even though this region is similar from a pressure difference standpoint between reference and 3D printed fans, that is not the case for the radiated sound field.

CONCLUSIONS

Three 3D printed fans implemented in this study showcased small deviations with regards to their manufacturing assessment. Differences regarding the characteristic curve of the fans fell within measurement uncertainty across different rotational speed, while respective efficiency curves demonstrated qualitative agreement. It would be of further value to repeat the unconclusive aerodynamic performance measurements at the separate testing facility, to minimize the uncertainty of the latter parameter. The acoustic performance of fans, including capturing of low-frequency phenomena, total SWL and directivity, across the sound characteristic map adds to the repeatability of the study.

Compared to the reference data [1], comparison of aerodynamic performance showed good agreement at the design point, including the location of maximum efficiency and the levels of pressure difference. With regards to the acoustic performance qualitative agreement was achieved for the frequency range studied at the design point. Tonal components due to BPF and maximum amplitudes due to tip clearance were reproduced at the measured spectra. In addition, the estimated total SWL adds to the overall reproducibility. Comparison of the total SWL over the sound characteristic curve at design rotational speed deduced quantitative agreement close to the design flow rate and low flow rates. However, significant deviations were observed at the stall region, despite the reasonable reproducibility of the aerodynamic characteristic curve. This promotes the need to further investigate the inflow conditions at this point as well as the acoustic's environment effect, which may contribute.

ACKNOWLEDGEMENTS

Test engineer Torbjörn ÅGREN is acknowledged for helping with the setup and calibration of the acoustic measurements. Thanks to Principal CFD Analyst Sassan Etemad for managing the preparation and operation of the fan test rig facility during the measurement campaign.

BIBLIOGRAPHY

[1] Florian ZENGER, Clemens JUNGER, Manfred KALTENBACHER and Stefan BECKER. "*A Benchmark Case for Aerodynamics and Aeroacoustics of a Low Pressure Axial Fan*" SAE Technical Paper. Warrendale, PA: SAE International, June 15, **2016**

[2] Mikael KARLSSON and Sassan ETEMAD. "*Installation Effects on the Flow Generated Noise from Automotive Electrical Cooling Fans*" SAE Technical Paper Series, no. 2020, **2020**

[3] Sassan ETEMAD and Peter GULLBERG. "*Validation of URANS Simulation of Truck Cooling Fan Performance*" American Society of Mechanical Engineers Digital Collection, **2015**

[4] The International Organization for Standardization (ISO), "*Acoustics — Determination of sound power levels and sound energy levels of noise sources using sound pressure — Engineering methods for an essentially free field over a reflecting plane.*" ISO 3744, Nov. **2010**

[5] Felix CZWIELONG, Florian KRÖMER and Stefan BECKER. "*Experimental Investigations of the Sound Emission of Axial Fans under the Influence of Suction-Side Heat Exchangers*" In 25th AIAA/CEAS Aeroacoustics Conference. American Institute of Aeronautics and Astronautics. Accessed December 23, **2021**

[6] Tao ZHU and Thomas CAROLUS. "*Experimental and Numerical Investigations of the Tip Clearance Noise of an Axial Fan Using a Lattice Boltzmann Method*," Conference paper: FAN 2015, Lyon, France, 15–17 April, **2015**